

# Properties of Vacuum Arcs Generated by Switching RMF Contacts at Different Ignition Positions

---

*A. Lawall<sup>1</sup>, E. D. Taylor<sup>1</sup>, F. Graskowski<sup>1</sup>,  
S. Gortschakow<sup>2</sup>, St. Franke<sup>2</sup>, D. Gonzalez<sup>2</sup>, R. Methling<sup>2</sup>, D. Uhrlandt<sup>2</sup>*

*<sup>1</sup>Siemens AG, Berlin, Germany*

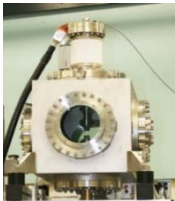
*<sup>2</sup>Leibniz Institute for Plasma Science and Technology, Greifswald, Germany*

# Outline



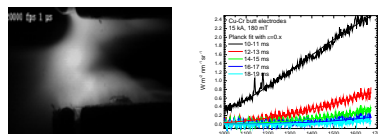
- Introduction

- Motivation



- Experimental setup

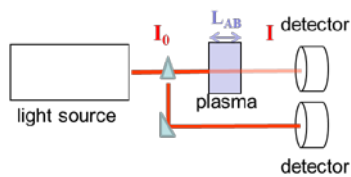
- Results and discussion



- Arc dynamics

- Surface temperature measurements

- Vapour density measurements



- Summary

# Introduction

## Vacuum interrupters



- outstanding insulation properties
- simple design, small number of components
- environmentally friendly operation – zero emission (no harmful gases, no light emission, no waste products)
- maintenance-free

## High-current operation

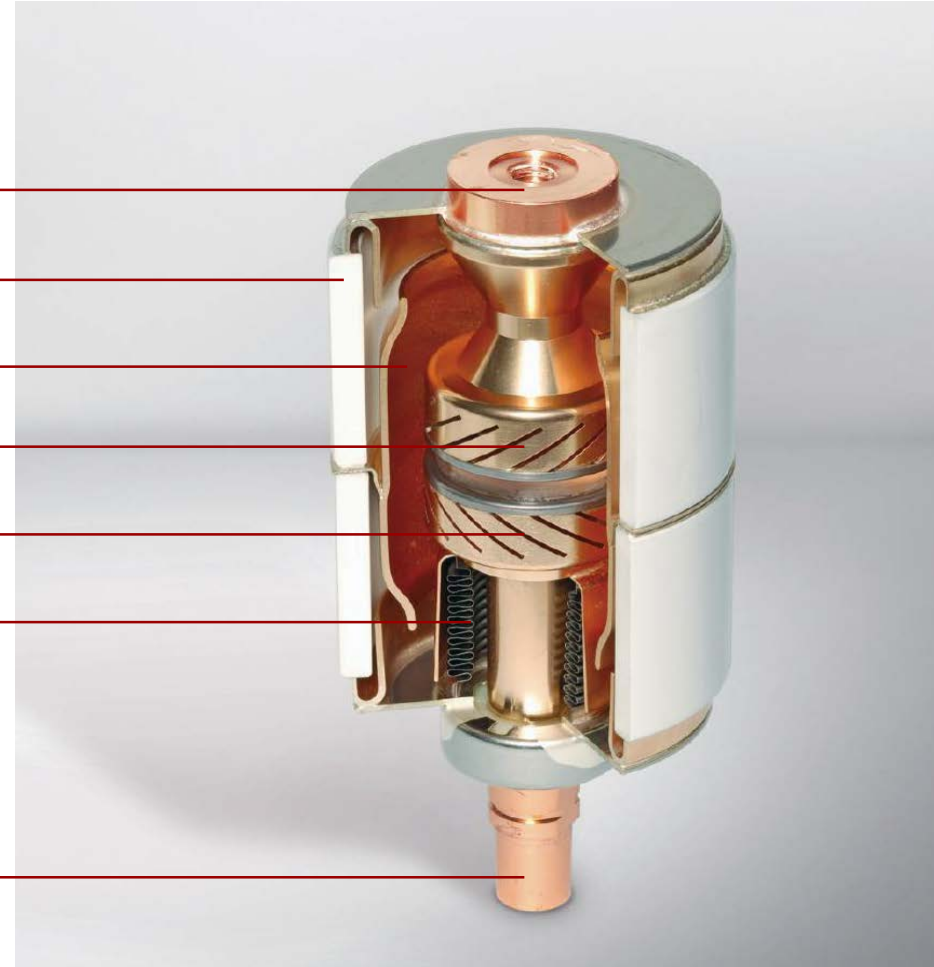
- strong electrode melting and evaporation
- measures of for reduction of thermal load necessary
- use of magnetic filed for arc control

## Two basic operation principles

- radial magnetic field (RMF) contacts: arc rotation over the electrode surface (constricted arc)
- axial magnetic field contacts (AMF): expansion of the arc column over most of the electrode surface (diffuse arc motion, and thereby the performance of the contacts.

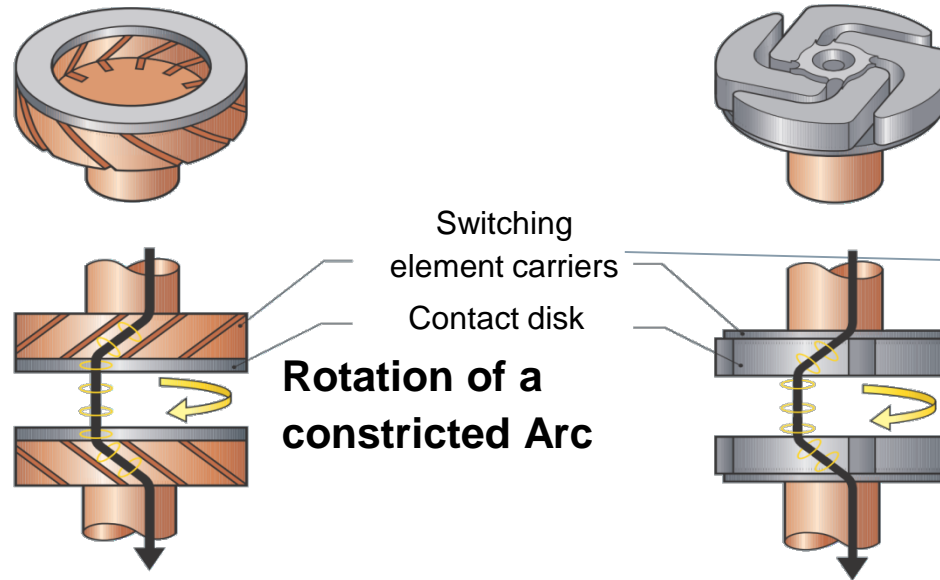
## Introduction: vacuum interrupter design

- Terminal disc
- Insulator (ceramics)
- Arcing chamber made of copper
- Fixed contact
- Movable contact
- Metal bellows
- Operating and connecting bolt

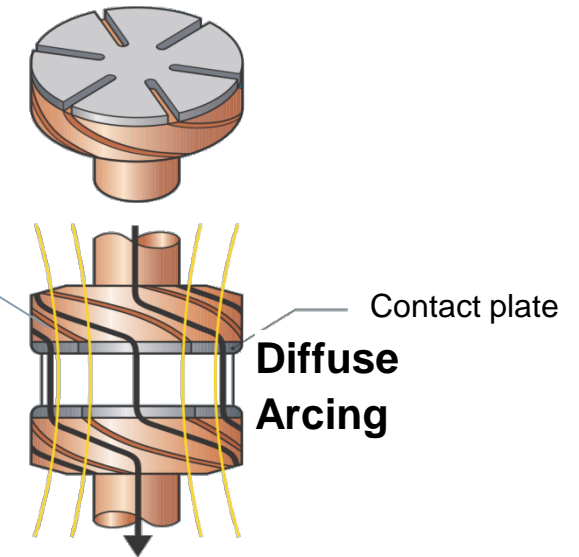


# Introduction: vacuum arc controlled by magnetic fields

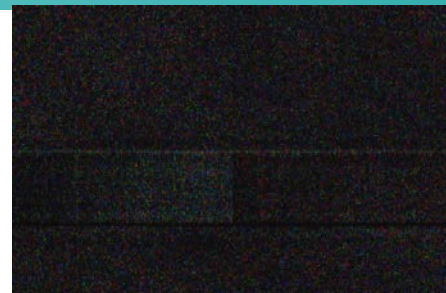
## Radial magnetic field contact (RMF)



## Axial magnetic field contact (AMF)



The contact geometry & magnetic field creation have a decisive influence on the switching capacity of a vacuum interrupter. Various contact geometries are used depending on the current & voltage ratings.



12.57 ms 20000 fps 20  $\mu$ s

# Motivation

---

## Open questions

- Influence of initiation behavior of the drawn arc on
  - arc motion
  - arc characteristics during the active phase
  - post-arc parameters

## Focus on

- arc dynamics
- anode surface temperature after current interruption
- neutral vapor density after current zero crossing

## Experimental setup: model vacuum interrupter



commercial vacuum interrupter

- Typical volume 0.5 l
- Stroke 5 – 20 mm
- Operation velocity 0.5 - 2 m/s



model vacuum interrupter

- Volume 52 l
- Mountings for various electrodes
- Stroke 5 - 25 mm
- Operation velocity 0.5 - 4 m/s

## Experimental setup: electrodes

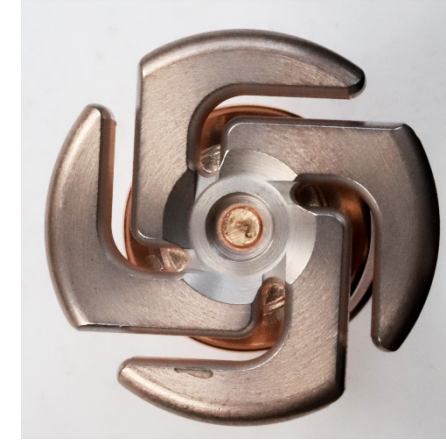


type A



type B

cathode

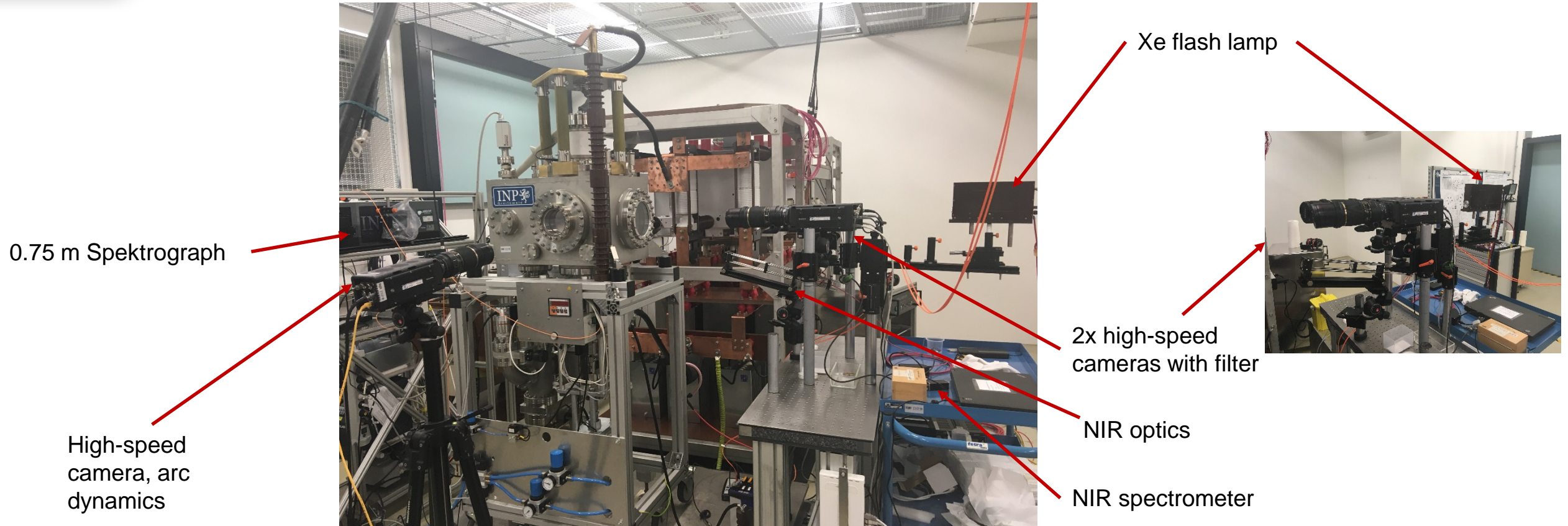


anode

- CuCr 60/40,  $\varnothing$  34 mm
- Defined ignition positions on movable electrode (cathode)
- Two distinguished positions – close outer boundary and close to the center

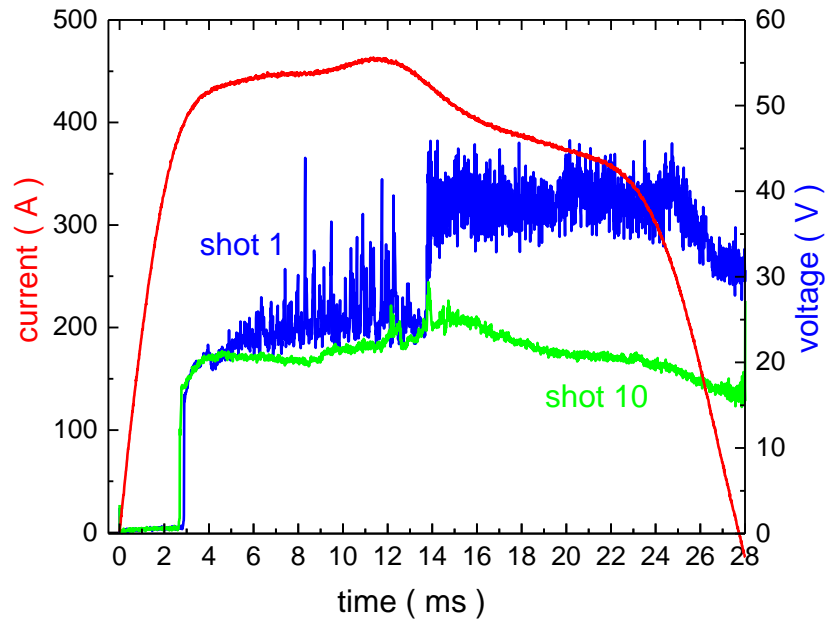


## Experimental setup: diagnostics

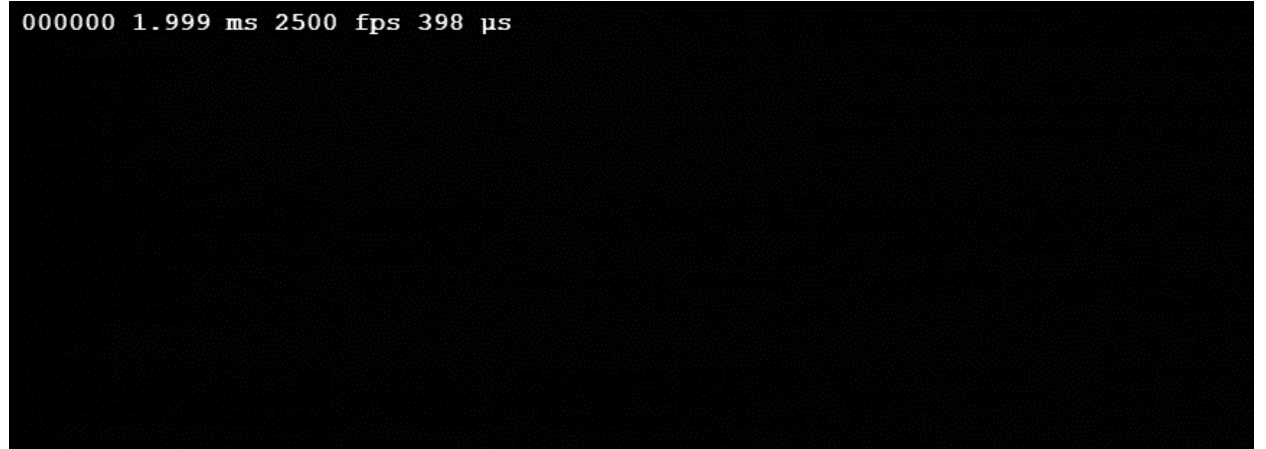


- Broad use of optical diagnostics: non-invasive methods, quantitative characterization of arc plasma and electrode surface

## Results: electrodes conditioning



electrical signals



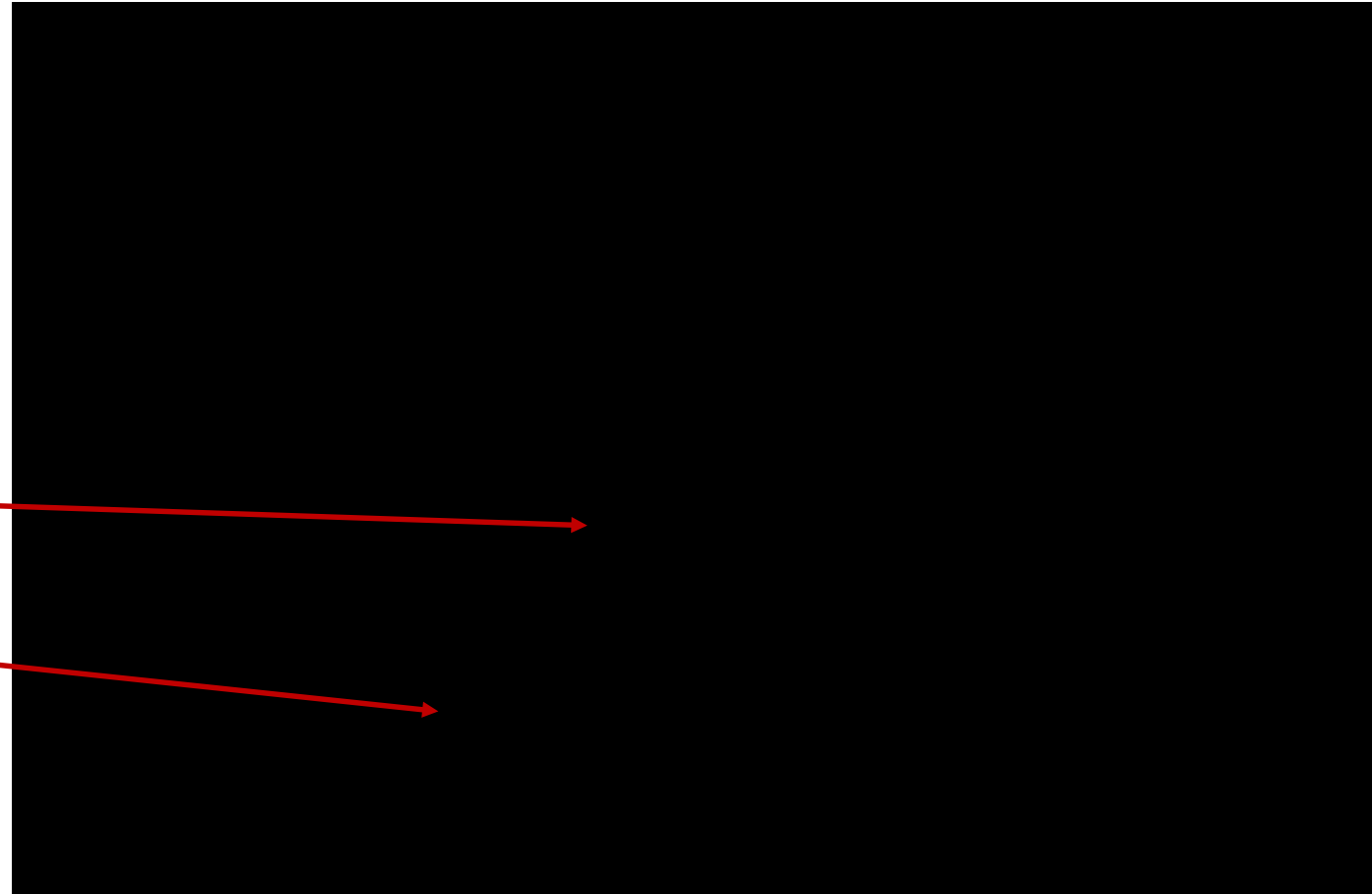
video

- Diffuse arc at pulsed DC operation, 20 ms, 430 A, 10 shots
- Control over the shape of voltage curve and pressure increase inside the chamber after the shot – ca  $2 \times 10^{-5}$  mbar after 1<sup>st</sup> shot, ca  $2 \times 10^{-6}$  mbar after 10<sup>th</sup> shot (measured at the instant of 20 seconds after shot)

## Results: arc dynamics

constriction

contact  
separation

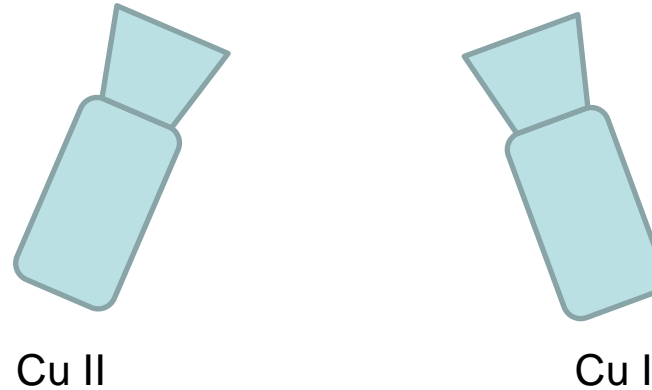


diffuse arc    moving constricted arc    diffuse arc

- Ignition at desired position (outer boundary, type A)
- Arc movement starts after appearance of an anode spot and arc constriction
- 2 rotations per ms at present experimental conditions
- Longer residence time in central part of electrode in case of ignition position B

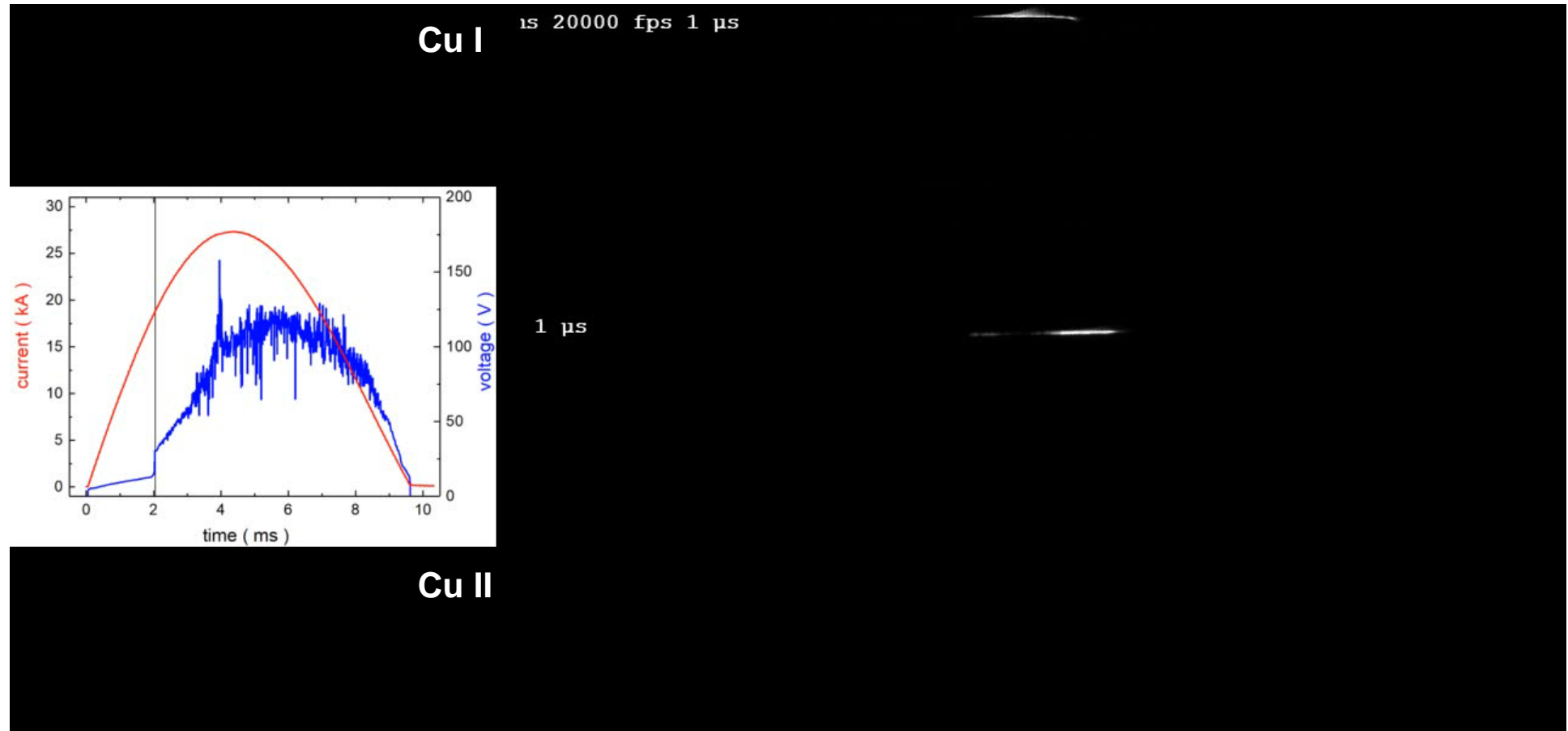
## Results: arc dynamics

Acquisition with narrow-band filter (MIF, 1 nm FWHM) 521 nm (Cu I) and 494 nm (Cu II)



- Focus on distinguishing between ion and atom dynamics

## Results: arc dynamics



- Pronounced differences in spatial distribution of atoms and ions

## Results: arc dynamics



- Higher atomic line radiation intensity at the beginning
- Increasing intensity of ionic lines with progressing time
- Localization of atomic line radiation in the broader regions close to the electrode surface
- However, no differences between studied ignition positions found



# Results: anode surface temperature



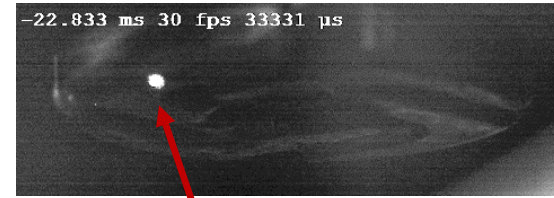
NIR 900-1600 nm

+

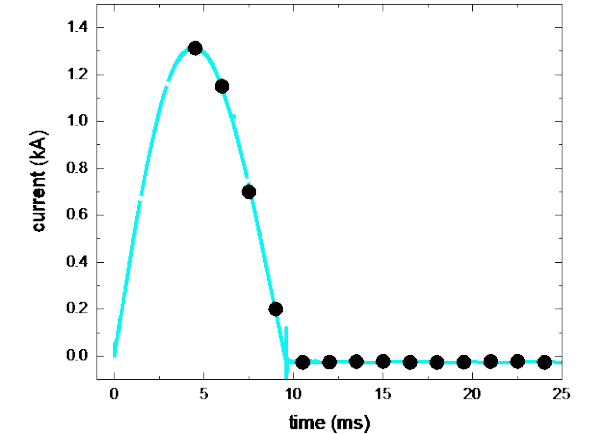


NIR optics

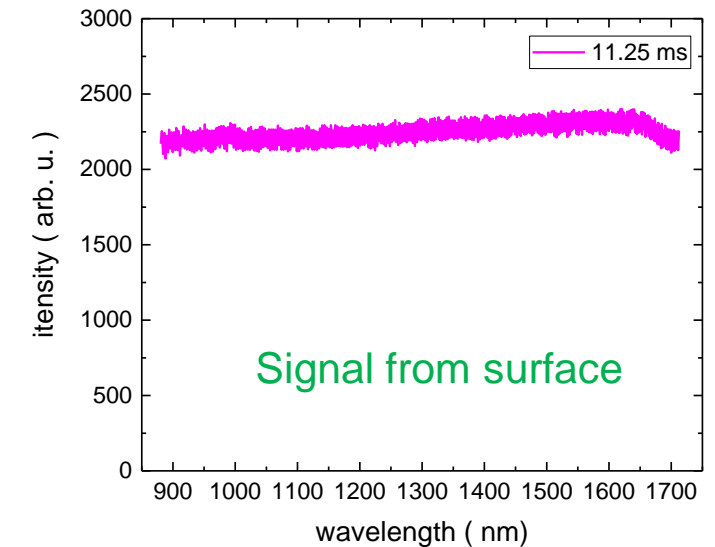
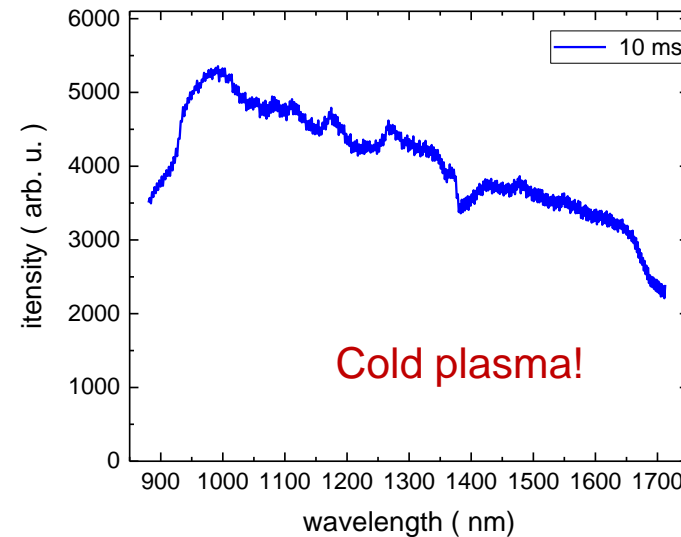
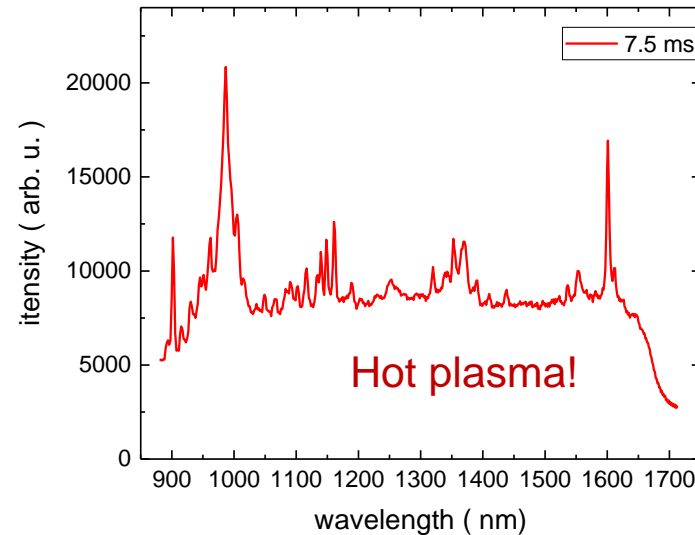
=



measuring point

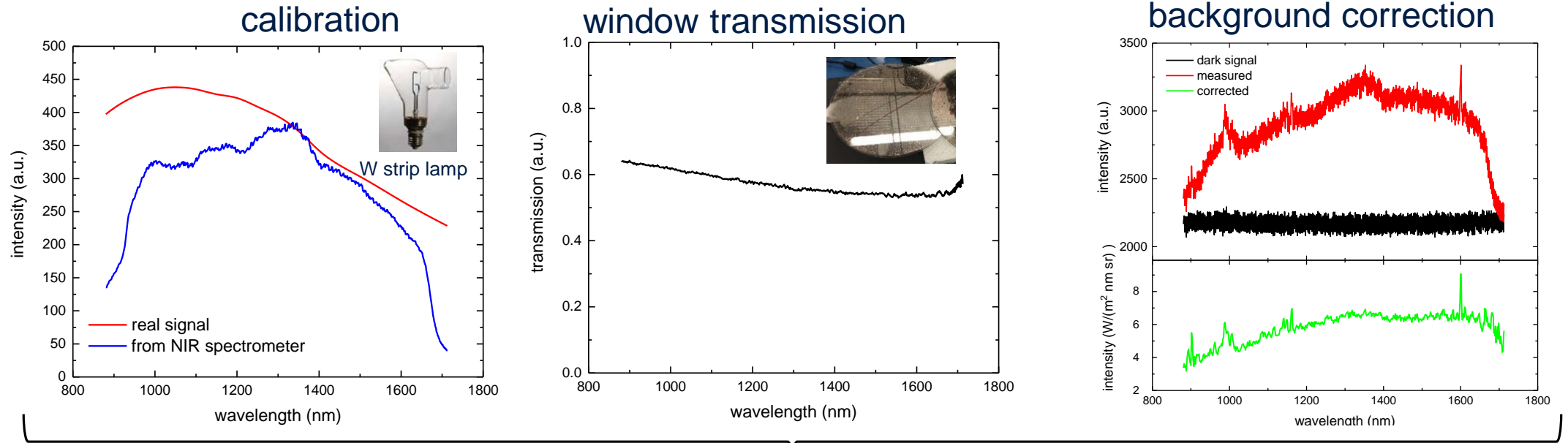


acquisition times



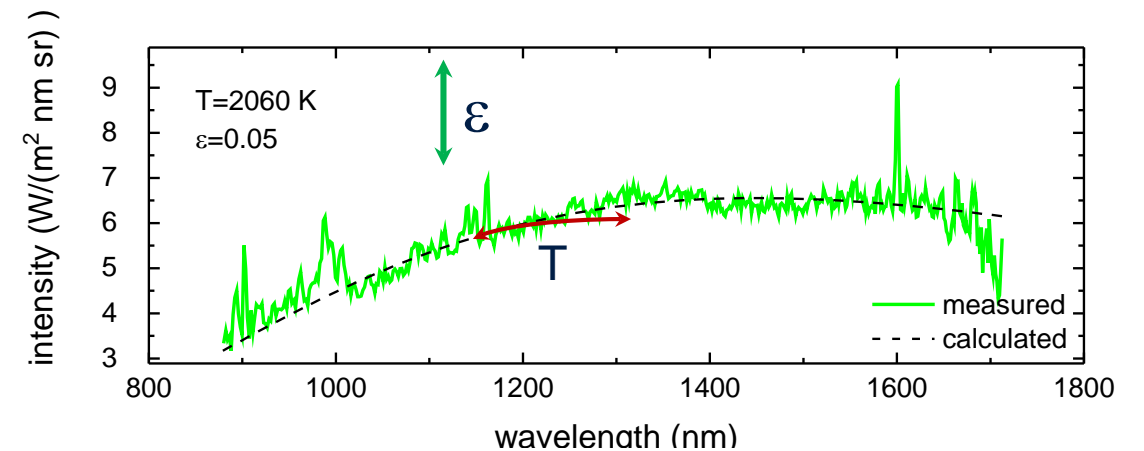
- Evaluation of NIR spectra emitted by hot electrode surface

# Results: anode surface temperature



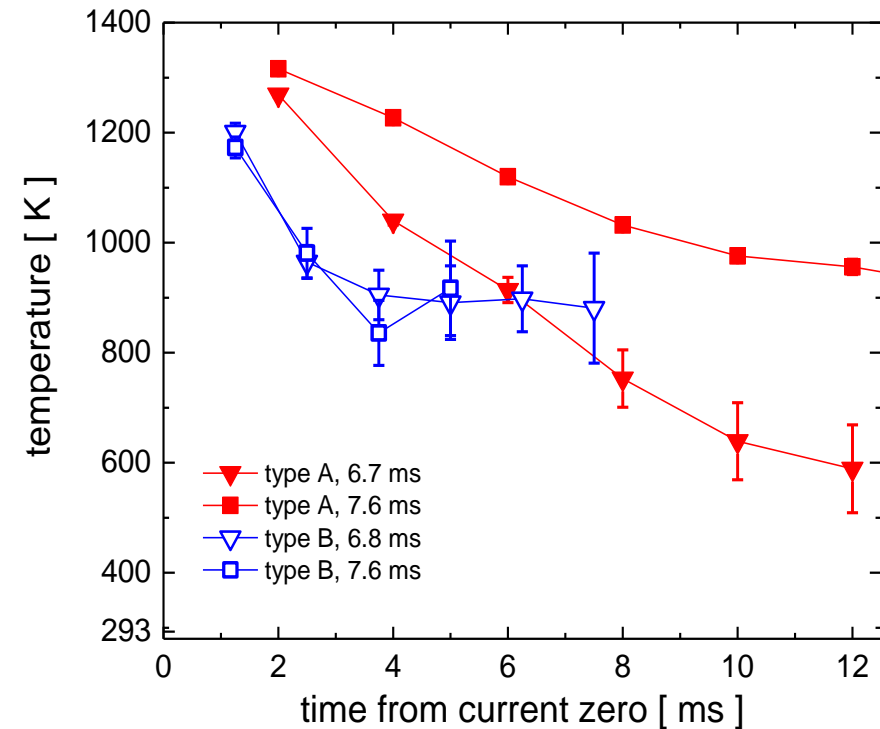
determination of  $T$  and  $\varepsilon$  from Planck fit

$$B_{\lambda}(T) = \varepsilon(\lambda, T) \frac{2hc^2}{\lambda^5} \cdot \frac{1}{e^{\frac{hc}{\lambda \cdot kT}} - 1}$$





## Results: anode surface temperature

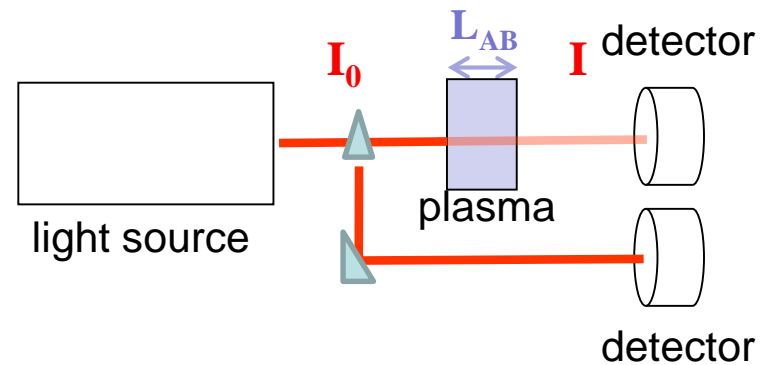


- Initial temperature in the range between 1200 K and 1400 K
- Higher temperature at longer arc duration
- Higher temperature in case of position A probably due to higher total residence time of the arc at this position

# Results: vapour density

## Principle of absorption spectroscopy

- Light source and detector



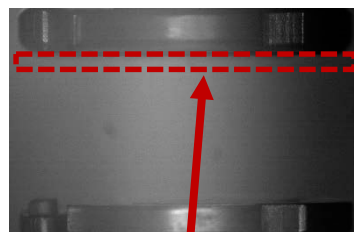
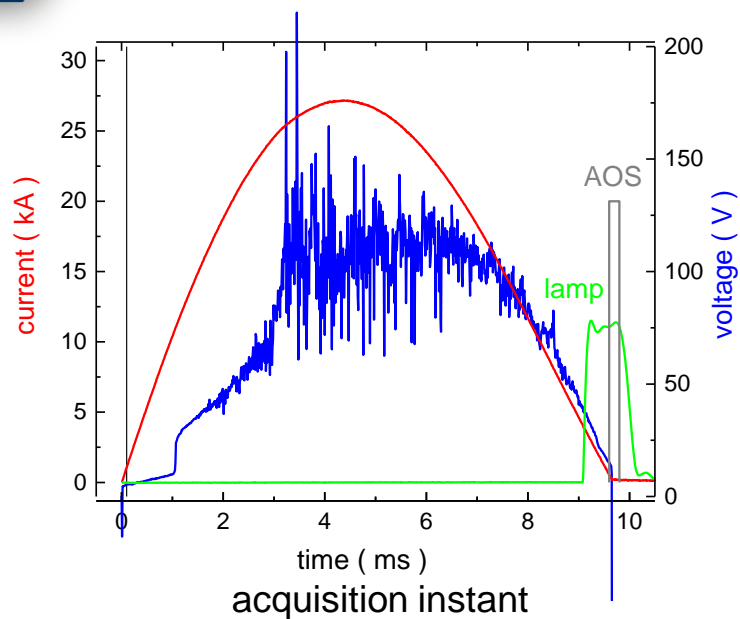
- Optical thickness

$$\tau(\lambda_L) = -\ln \left( \frac{I(L_{Ab}, \lambda_L)}{I_0(\lambda_L)} \right)$$

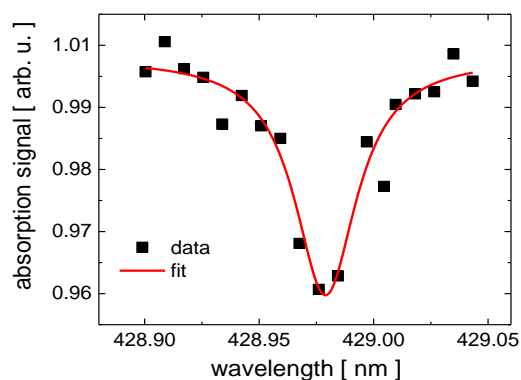
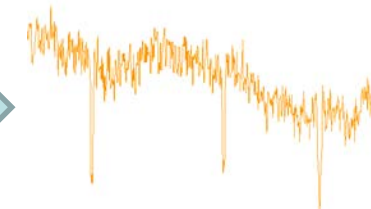
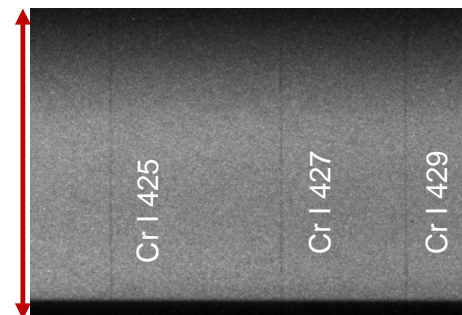
- Density of absorbing species

$$\frac{1}{L_{AB}} \int_0^\infty \tau(\lambda_L) d\lambda = \frac{\pi e^2 \lambda_0^2}{\epsilon_0 m_e c^2} N_l f_{lu}$$

# Results: vapour density

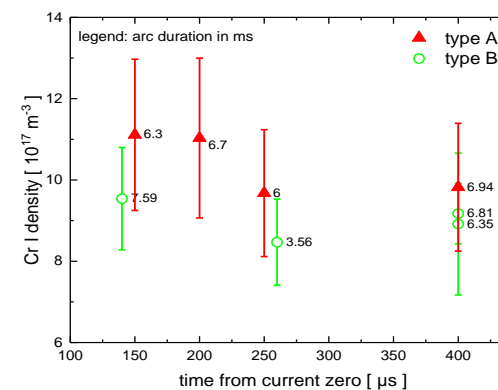


Anode



central wavelength $\lambda$	oscillator strength $f_{lu}$
425.435	0.11
427.481	$8.42 \times 10^{-2}$
428.973	$6.23 \times 10^{-2}$

$$\frac{1}{L_{AB}} \int_0^{\infty} \tau(\lambda_L) d\lambda = \frac{\pi e^2 \lambda_0^2}{\epsilon_0 m_e c^2} N_l f_{lu}$$

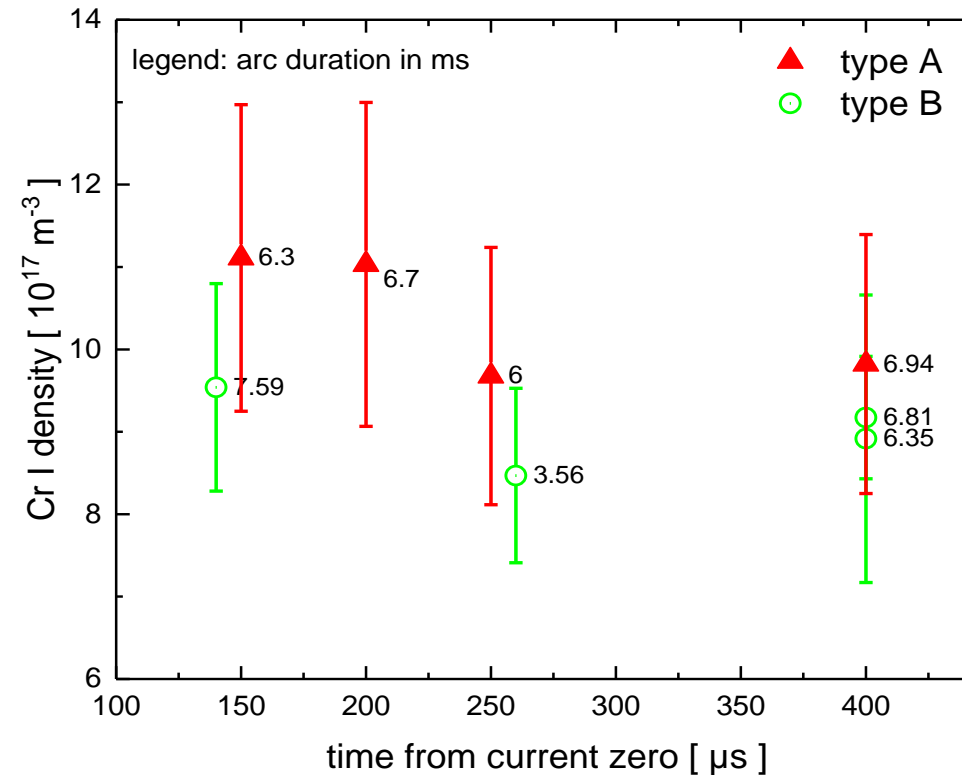


line fit

data processing

density

## Results: vapour density



- Slow density decay within first 400  $\mu\text{s}$  after current interruption
- Higher chromium density in case of longer arc duration
- Higher chromium density in case of position A due to higher anode surface temperature

## Summary

---

- Clear influence of initiation behavior of the drawn arc on arc parameters was found
- Higher electrode temperature in case of the electrodes with position A (ignition point near the outer boundary of the electrode)
- Consequently higher density of chromium vapor, even though the arc duration was longer.

# Thank you very much for your attention!



Dr. Sergey Gortschakow

Leibniz Institute for Plasma Science and Technology

Address: Felix-Hausdorff-Str. 2, 17489 Greifswald

Phone: +49 - 3834 - 554 463, Fax: +49 - 3834 - 554 301

Email: [sergey.gortschakow@inp-greifswald.de](mailto:sergey.gortschakow@inp-greifswald.de)

Web: [www.leibniz-inp.de](http://www.leibniz-inp.de)

## Optical diagnostics: advantages and disadvantages

- Clear advantages of optical methods
  - non-invasive
  - qualitative and quantitative measurements possible
  - high spatial resolution – local properties
  - high temporal resolution – dynamics
  - applicable in a wide parameter range due to variability of methods
- Some disadvantages of optical measurements
  - optical access to the object necessary
  - radiation intensity must be sufficient
  - distortions in the optical pathway through hot fluxes and plasma itself
  - costs of the devices, complex apparatus and evaluation methods